SOLAR ACTIVITY, EL NINO-SOUTHERN OSCILLATOIN AND RAINFALL IN INDIA.

Prof. Ernest C. Njau*

Abstract:

Some new connection between rainfall in India and solar activity is illustratively established. Being closely associated with rainfall in India, El Nino events and the Southern Oscillation are also studied by critically analyzing their occurrence patterns since 1900 and establishing possible relationship between these patterns and solar activity. On the basis of this critical analysis, some new scientific findings are arrived at, including a prediction that the next two El Nino events will expectedly occur during the 2007 – 2009 and 2010/11 – 2012/13 periods. This prediction is further re-confirmed / re-ascertained using the theory of El Nino events. Some new switching/changing patterns in the amplitude envelopes formed by variations in the southern Oscillation (S and North Atlantic Oscillation (NAO) are also established. These patterns may be used to predict occurrences of major droughts in certain regions of the world. Finally it is established that the SO and some features in the NAO are basically caused by similar heat/temperature waves.

Key Words: Solar-Terrestrial Physics, Indian Rainfall, El Nino-Southern Oscillation (ENSO)

* University of Dar es Salaam, Dar es Salaam, Tanzania.

Introduction:

Variations or activities in the Sun (i.e. solar activity) are traditionally measured by the number of dark spots on the Sun's disc. These dark spots are called sunspots. It is now common knowledge that solar (or sunspots) activity varies cyclically or quasi-cyclically at a number of periods including 11 years, 22 years and others as illustrated in Fig. 1. Detailed theory and physical mechanisms which link solar activity and terrestrial climate have been published recently [3]. In this paper, we use the contents of the latter reference as a guide in establishing specific links between solar activity and rainfall in India. Since El Nino events generally influence rainfall in India, we go further by looking into possible ways of predicting occurrences of future El Nino events. A definition of El Nino (or El Nino event) is given later on in this paper.

Analysis:

Fig. 2 shows variations in the summer monsoon (June – September) rainfall over India from 1881 to 1980. In line with Ref. [3], the rainfall variation patterns in Fig. 2 clearly adopt one of two modes at a time. In one of these two modes, the envelope of the variation patterns is generally sinusoidal or quasi-sinusoidal (e.g. see Fig. 2 from about 1900 to about 1960). Let us hereinafter refer to this particular variation mode as "sinusoidal mode" or simply SM. In the second mode, the envelope o the variation patterns are shaped into a series of nodes and antinodes (e.g. see Fig. 2 before 1900 and after 1960). Let us hereinafter refer to this variation mode as "node-antinode mode" or simply NM.

It is interesting to note that the rainfall variation patterns in Fig. 2 change form SM to NM or vice versa only at a maximum or minimum of the solar activity curve in Fig. 1(b). Indeed this observation applies also to all annual rainfall variations at individual stations or regions in India. As a representative exampl3e in this case, look at the annual rainfall variations at Madras from 1813 to 1955 shown in Fig. 3. As implied above, these rainfall variations (see Fig. 3) also change from SM to NM or vice versa only at a maximum or a minimum of the solar activity curve in Fig. 1(b). Other meteorological parameters in India also seem to vary in compliance with the solar activity connection reported above in connection with rainfall. For example, variation in total ozone over 5 stations in India from 1954 to 1976 also display a switch from SM to NM at about 1960, the time location of a maximum of the curve in Fig. 1(b) (see Ref. [6]).

Following the observations given in the previous paragraph, we carried out extensive analyses of records of global meteorological parameters specifically to find out if they too exist in a series of SM and NM modes. Surprisingly we discovered that ALL records of global meteorological parameters exist in a series of SM and NM modes as typically illustrated in Fig. 4. This figure displays a change from NM to SM in 1971/72, with the post – 1971/72 SM mode having a period equal to that of the 11-year sunspot cycle. Results presented elsewhere [7] shows that the SM in Fig. 4 continues consistently and with a period of 11 years up to (at least) 2003. On the basis of the mode-changing sequence given in Ref. [3], the post – 1971/72 SM in Fig. 4 is expected to change to NM at or close to the next minimum of the dashed-lone curve in Fig. 1(a).

A well known meteorological phenomenon that is closely related to rainfall in India is the El Nino or El Nino event [4]. By definition, an El Nino is the phenomenon in which the

entire eastern equatorial Pacific Ocean dramatically warms up by several °C . The opposite of this phenomenon is called anti-El Nino or La Nina. Since El Nino events are strongly associated with global meteorological parameters whose variation patterns reflect two different modes (e.g. see Fig. 4 and Refs. [3, 6, 7, 10 – 12]), it would seem that occurrence patterns of El Nino events could probably reflect two different modes as well. This point of view is rigorously pursued below.

We collected from Refs. [4, 8, 9], a record of all the El Nino events that have occurred from 1900 up to the present time. This record is summarized in Table 1 together with timings of minima and maxima of 11- year sunspot cycle.

An analysis of the data in Table 1 shows that all the El Nino events are clustered at / around maxima and minima of the 11-years sunspot cycle with exception of the 1933 minimum and 1947 maximum. The reasons for this exception are as follows. For the 1933 minimum, no El Nino would take place at or near it because this minimum coincides with the time at which the locus of instantaneous solar activity level crosses the equilibrium level of solar activity. In fact, there was no El Nino event between 1929 and 1939. More details on this are found in Ref. [10]. For the 1947 maximum, no El Nino would occur at or near this maximum because 1947 is the time during which the dashed line curve in Fig. 1(a) changes its frequency. It is basically for this reason that there was no El Nino event between 1941 and 1951. Details on this aspect may be found in Refs. [3, 7, 10-12].

If we now disregard the 1933 minimum and the 1947 maximum in Table 1 for the reasons just given above, the occurrence patterns of the El Nino events since 1900 display two modes. If the time location of a maximum or minimum of the 11-year sunspot cycle is denoted by T, then the two modes are given as follows:-

MODE A: In this mode, El Nino events occur only within the period $T \pm 3$ years, for all individual values of T, where n is a positive integer. This mode operated up to 1971/72 with n=3, and coincides with a rising phase of the oscillation in Fig. 1(b).

MODE B: In this mode (which operates after 1971/72), El Nino events occur only within the period T to T +m years, for all individual values of T, where m is a positive integer. In this particular case, m=2. Note that this particular mode coincides with a falling phase of the oscillation in Fig. 1(b).

Table 1: Timing of maxima and minima o fthe 11 year sunspot cycle as well as El Nino events since 1900

Year of 11-year sunspot cycle maximum		1906		1917		1928		1937		1947		1957		1969		1980		1990		2000/1		2010/11
Year of 11-year sunspot cycle minimum	1901		1913		1923		1933		1944		1954		1964		1976		1986		1996		2007	
Year at which El Nino starts	1902	1905	1911 1914	1918	1925	1929	*	1939	1941	**	1951 1953	1957	1963 1965	1969 1972	1976	1982	1986	1992	1997	2002	?	?

* Year 1933 is the time at which the instantaneous solar activity level crosses the solar activity equilibrium line [10], thus eliminating any chance of El Nino formation according to the theory in Ref. [16].

** Year 1947 is the time at which the dashed curve in Fig. 1 changes period from ~22 years to a larger value, thus eliminating any chance of El Nino formation according to the theory in Ref. [16].

Theoretical justification for existence of Mode A and Mode B is given later on in the paper. Note specifically that during Mode A, a maximum or minimum of the 11-year El Nino events. This specific situation occurred in connection with the II-year sunspot cycle minima at years 1913, 1954 and 1964 (see Table 1).

If we want to predict occurrences of future El Nino events using Mode B, we must first find out for how long from now this mode will remain valid. Such a finding may be obtained from analysis of long-term records of the Southern Oscillation (SO). This is the case because the EI Nino is not only closely connected to the SO, but also both the EI Nino and the SO are two aspects of one global -scale oscillation in the combined ocean-atmosphere system [4]. The SO (which is defined as a seesaw oscillation of surface air pressure in the tropical Pacific and Indian Oceans) is measured and recorded using an index called Troup Southern Oscillation Index (SOI).

Looking at the SOl graphical representations in Fig. 5 and Fig. 6 as well as some pre-1900 El Nino records, it is clear that:-

a) The rising phase of the dotted curve in Fig. 5 coincides with Mode A while the falling phase of the same curve coincides with Mode B. Note the absence of El Nino events between 1929 and 1939 (see Fig.5), which has already been explained.

b) The falling phases of the dotted oscillation in Fig. 5 coincide with relatively amplified NM modes in Fig.6 while the rising phases coincide with relatively smaller NM modes in Fig. 6.

c) The conversion from NM to SM in the variations shown in Fig. 7(b) (see Ref. [12]) coincides with the conversion of NM to SM in Fig. 8.

d) The changes in amplitude -modulation envelope pinpointed by arrowed lines in Fig. 8 precede corresponding changes in Fig.6 by not more than 4 years.

e) In either Fig. 6 or Fig. 8, the changes pinpointed by arrowed lines take place at a period of36 years. This period is equal to that of the 35-40 years solar cycle.

f) During Mode A, both Fig. 6 and Fig. 8 have NM. But during Mode B, Fig. 6 has NM while Fig. 8 has SM. Note that apart from the dotted NM in Fig.8, this figure also displays dashed NM at periods of ~11 years and ~22 years.

g) The minimum and maximum of the dotted curve in Fig.'s are at about 6 years after the ~ 1900 minimum in Fig. 1 (b) and at about 15 years after the ~ 1960 maximum in Fig. 1 (b), respectively.

All the observations (a) to (g) listed above obey (or take place according to) the already accepted theory [3,11,19] which governs NM and SM modes in meteorological/climatic parameters. Therefore these observations can be taken up without the need to present more rigorous statistical analysis. In the case of the NM and SM modes shown in Figs. 6 and 8, for example, such statistical analysis would require longer records which are not available at all. Mostly on the basis of points (d), (e) and (f) given above, we can assume that the SM in Fig. 8 and the last NM in Fig. 6 will exist up to at least about year 2014. This implies that the currently existing Mode B is expected to persist up to at least the

latter year. Therefore, we can fill the two blocks having question marks in Table 1 with the following prediction which is based on Mode B:-

The next two El Nino events are expected to occur during the 2007 -2009 period (but more probably during 2007/8) and the 2010/11 -2012/13 period (but more probably during 2012/13).

Alternatively this prediction can be simply established using the EI Nino theory [16] as follows. According to the latter theory, an EI Nino results when: (i) Overlapping peaks of the seasonal heat wave and at least two of certain eastward-moving heat waves (which are internal modes of the equatorial surface-atmosphere system) at periods 2-3 years, $\sim 5\frac{1}{2}$ years and ~ 11 years, each having ~360 longitude degrees zonal wavelength cross the eastern equatorial Pacific Ocean; and (ii) The heat content in the overlapping peaks just mentioned is significantly focused onto a stretch of the eastern equatorial Pacific ocean by the concave-shaped lining of the lofty Rocky-Andes mountains. Simple analysis shows that the peaks of the seasonal heat wave and at least two of the 2-3 year, $\sim 5\frac{1}{2}$ year and 11-year heat waves overlap over the eastern equatorial Pacific Ocean after every $\sim 5\frac{1}{2}$ year and 11 years. Also the peaks of all the four heat waves overlap over the eastern equatorial Pacific Ocean after every ~11 years. Hence during an SM mode in Fig. 6, these four heat waves interact additively so that EI Nino events occur at a period of $\sim\frac{1}{2}$ of the 11-year sunspot cycle period. This theoretical conclusion, which is verified in Table 1, forms the basis of the prediction established earlier in this paper. The theoretical conclusion just mentioned may be used to build up a theoretical justification for the existence of Mode A and Mode B.

According to the theory of EI Nino events mentioned above, occurrence of EI Nino events tends to be "erratic" in Mode A whenever the magnitude of the gradient of the curve in Fig. 7 (b) is fairly large for positive values of SN frequency. This condition took place in Fig.7 (b) between 1910 and 1919 as well as between 1950 and 1970. And as can be verified in Table 1, occurrence of El Nino events became relatively "erratic" between 1910 and 1919 as well as between 1950 and 1970. Now when the curve in Fig. 7(b) is along (or meanders closely about) the zero level, the resulting Mode B offers relatively simple way/chance of predicting associated El Nino events. It is on this basis that the next two major El Nino events have been predicted in this paper.

The prediction just mentioned is of importance for the Indian people and their economy since insufficient rainfall in India tends to follow the peak of an El Nino while sufficient rainfall in India tends to occur during an anti-EI Nino [4]. The prediction methodology used in this paper is exactly the same methodology which was used in the author's 1999 paper [15] to successfully predict the occurrence of the 2002 EI Nino event. Finally it is worth noting that the prediction established in this paper has also been consistently arrived at after Figs. J to 7 and Table 1 were analysed separately using several long-standing techniques as well as modem techniques (e.g. the wavelet analysis method).

One of the most interesting findings of this paper is existence of the changes pinpointed by arrowed lines in Fig. 6 and Fig. 8 whose apparent periodicity is 36 years. Physical interpretations of these 36-year changes will be given latter on in the paper.

A close comparison of Fig. 6 and past severe droughts over East Africa yields the following. A severe drought over East Africa starts ~ 4 years after a node in Fig. 6 and proceeds for more than 6 years except for interruption of a major El Nino event some 10-11 years after the node. Where a regular NM mode is involved, the starting point just follows an El Nino event. Now each arrow in Fig. 6 is preceded by a node by 11-13 years. Since the arrows in Fig. 6 are uniformly separated by 36 years, the next arrow is expected to be located at year 2014. Therefore the next node (see Fig. 6) is expectedly located in year 2001 -2003. On the basis of the account just given above, the next major drought over East Africa is expected to start somewhere over the 2005 -2007 period, just following an expected El Nino event. The latter EI Nino event seems to be that already predicted earlier in the paper for year 2007/2008 using a different method. And finally the next major El Nino event is expected to occur some 10-11 years after the 2001-2003 node, that is, during 2011-2014. Note that a major EI Nino has been predicted earlier in the paper for year 2012/2013 using a different method.

Detailed Interpretation of Figures 6 and 8:

In this section we present a deeper analysis of the graphical patterns in Figs. 6 and 8. As a starting point in this case, we give more detailed definitions of the Southern Oscillation and North Atlantic Oscillation. The Southern Oscillation (which was discovered in 1923) is a seesaw oscillation in surface atmospheric pressure between the southeast Pacific subtropical high and the region of the low pressure stretching across the Indian ocean from Africa to northern Australia. An index for the Southern Oscillation (which is called "Troup Southern Oscillation Index (SOl)) is defined as follows:

$$SOI = \frac{10\left(PA\left(Tahiti\right) - PA\left(Darwin\right)\right)}{SD} \qquad \ldots\ldots\ldots\ldots\ldots (1)$$

where PA = monthly see -level pressure anomaly and SD = standard deviation of the pressure differences for that month over the reference period. On the other hand, the North Atlantic Oscillation (which was discovered between 1923 and 1933) is a seesaw oscillation in surface atmospheric pressure between the North Atlantic regions of the subtropical- high surface pressure (centred near the Azores) and subpolar -low surface pressure (extending south and east of Greenland), Just as the Southern Oscillation is measured by the SOl, the North Atlantic oscillation is measured by an index called "North Atlantic Oscillation Index (NAOI)". In fact, the Southern Oscillation (SO) and the North Atlantic Oscillation (NAO) are two major oscillations of the planetary atmospheric pressure fields. The other major oscillations are: the Pacific -North American Oscillation, the North Pacific Oscillation, and the Eurasian Oscillation.

On the basis of equation (1) and the relationship between atmospheric pressure and temperature/heat, the NM modes in Fig. 6 are apparently caused by a mixture of large zonally moving heat/temperature wave (hereinafter simply called "large wave" or "L

wave") at zonal wavelength approximately equal to $\frac{1}{n}x$ (equatorial circumference) where n=1,3,5, and other zonally moving heat/temperature wave(s) (hereinafter simply called "other waves(s)" or "O wave(s)") at relatively smaller zonal wavelengths. According to Ref. [16], the L wave and O waves stretch across the equator from pole to pole. A node in Fig. 6 coincides with the time at which a maximum or minimum of the L wave lies along the longitude midway between Darwin and Tahiti. Also each of the transition zones between adjacent NM modes in fig. 6 coincides with a time at which a zero level of the L wave is along the longitude midway between Darwin and Tahiti. This point is supported and verified by the fact that alternate arrows in Fig. 6 (i.e the 1906 and 1978 arrows) are at or near abnormally severe EI Nino events while the arrows between these alternate arrows are at or near relatively smaller EI Nino events. The account given above easily shows that the L wave drifts zonally at a speed of about 50 of longitude per year. Similar analysis applied to Fig. 5 shows that the SM modes in this figure are dominantly shaped by a large zonally moving heat/temperature wave with zonal wavelength equal to that of the L wave but with a relatively smaller zonal speed. All zonally moving heat/temperature waves that drive the Southern Oscillation are governed by the equation

$$V \approx \frac{360^\circ}{n} \qquad \text{.....(2)}$$

where V is zonal speed in longitude degrees per unit time and T is period in unit time. The waves essentially acquire zonal wavelength $\frac{360^\circ}{n}$ due to resonance conditions [19]. It is apparent that waves associated with the southern oscillation and the related El Nino events largely obey equation (2). Such waves have a range of periods (i.e. the periods of quasi -biennial oscillations, solar cycles ...etc.) as well as a range of zonal speeds [16]. The L wave is one of these waves.

Standard climatology textbooks (e.g. Ref. [4]) indicate that for ENSO modes, n=1 in equation (2), leading to the equation

$$VT \approx 360^\circ \qquad \text{.....(3)}$$

According to Refs. [3, 10, 11, 16], all large eastward -moving heat/temperature waves stretching sufficiently from north to south across the equator and whose peaks cross the American continent can give rise to El Nino events. But among all these waves, only those obeying equation (2) can (resonantly) drive the Southern Oscillation. This supports the well known view that the El Nino and Southern Oscillation phenomena are two aspects of one global -scale oscillation. Note that a series of large eastward-moving heat/temperature waves derived from the constant component of incoming solar energy quasi-continuously exist in the surface-atmosphere system at various periods [3, 4, 7, 10, 11]. It is from this series of waves that the waves which obey equations (2) and (3) are derived at the frequencies of solar cycles, quasi-biennial oscillations...etc.

Looking at the relationships between the structures in Fig. 6 and those in Fig. 8 given in the preceding section, it is clear that the dotted NM and SM modes in fig. 8 are caused

by physical interactions between northern hemisphere (heat/temperature) patterns and the L wave and 0 waves. This conclusion may be proved alternatively as follows. Theory shows that the 0 waves and L wave drift eastwards [3, 16, 19]. If the northern parts of the latter waves are responsible for the dotted NM and 8M modes ,in Fig. 8 through physical interactions with variations in the northern hemisphere, then:

(i) The arrows in Fig. 8 must precede those arrows in Fig. 6 by about 4 years. The truth from Figs. 6 and 8 is that the former arrows precede the latter arrows by about 4 years.

(ii) The zonal speeds (in longitude degrees per year) calculated from the structures in Fig. 6 must be equal to the zonal speeds calculated from the structures in Fig. 8. In fact the zonal speeds calculated from Fig. 6 are equal to those calculated from Fig. 8.

(iii) The abnormally severe EI Nino events at or near the first and third arrows in Fig. 6 must correspond to large "jumps" in the patterns in Fig. 8. This is what, is actually the reality.

(iv) The general periodicity reflected by the dotted NM and 8M modes in Fig. 8 must correspond to that reflected by the NM patterns in Fig. This is what, is actually the case.

From the signal processing point of view the NM modes in fig. 6 as well as the dotted NM and 8M modes in Fig. 6 as well as the dotted NM and 8M modes in Fig. 8, being representations of pressure differences between pairs of specific locations, are obviously caused by passages of pressure waves across the pairs of the specific locations. This is deduced purely from the shapes/patterns of the modes and their association with relevant signal processing and shaping techniques. The pressure waves just mentioned are derived from the Land 0 (heat/temperature) waves described in the text through well known temperature -pressure relationships in the atmosphere. Finally it is worth noting that the contents of this section explain and account for the ENSO -related precipitation anomalies over the globe very successfully.

Calculations involving the NM and SM modes in Figs. 6 and 8 as well as equation (2) show that each arrow in Fig. 8 coincides with the time at which a peak of the L wave crosses the region associated with the NAOI. Furthermore each of the NM and SM modes in Fig. 8 is spectrally different from any other mode. This point is verified as follows. Firstly the -1866-1902 NM mode and the 1902-1938 NM mode involve 11-year and 22- year latitudinally moving heat/temperature waves, respectively (see the dashd NM modes in Fig. 8). Secondly the 1938-1974 NM mode and the post -1974 SM mode do not involve II-year or 22-year waves, but they obviously differ from each other spectrally. It is clear, therefore, that each passage of an L wave peak across the region associated with the NAOI switches the NAO into a different NM or SM mode. By simple theoretical extrapolation, it is most probable that passage of an L wave peak across the region associated with any of the other major oscillations of the planetary atmospheric pressure fields switches that particular oscillation into a different NM or SM mode. Unfortunately we have not been able to collect enough records with which this theoretical extrapolation could be verified.

General Conclusion:

Some relationship has been established between solar activity on one hand and Indian rainfall, El Nino, the Southern Oscillation (SO) as well as the North Atlantic Oscillation (NAO) on the other hand. Both the SO and NAO are shown to be basically related through specific global heat/temperature waves. The relationship between solar activity and El Nino has been exploited and used to predict timings of the next two major El Nino events. Further investigations into the relationship mentioned above may yield results which can possibly be used to predict not only other future El Nino events but also severe droughts in some regions of the world.

Acknowledgements:

The author is very grateful to Profs. P. Ramanathan and R. Prasad as well as Dr. V. Balaram for useful comments on an earlier version of this paper.

References:

Paul M. and Novotna D., Phys. Rev. Lett., 1999, 83, 3406.

The curve-fitting toolbox at http://www.mathworks.com/nncurvefitting visited on 26/06/2005.

Njau E.C., Nuovo Cimento C., 2004, 27, 579.

Peixoto J.P. and Oort A.H, 1992."Physics of Climate", American Institute of Physics, New York.

UNESCO, 1963, "Changes of Climate", UNESCO, Paris.

Njau E.C., Nuovo Cimento C, 2006 (In the Press).

Njau E.C., Nuovo Cimento C, 2003, 26, 613.

Glantz M.H., Katz R. W. and Nicholls N. (Eds), 1991, "Teleconnections linking worldwide climate anomalies", Cambridge University Press, Cambridge.

Website http://www.cru.uea.ac.uk/tiemoo/floor O/theme.htm. visited on 14/06/2005

Njau E.C., Nuovo Cimento C, 2004, 27, 133.

Njau E.C., Nuovo Cimento C, 2003, 26, 23.

Njau E.C., Int. J. Renewable Energy, 2005, 30, 743.

Miller J.B., 1999, WMO Bulletin, 48, 49.

Houghton J. T., Meira Filho L. G., Callender B.A., Harris N., Kattenberg A. and Maskell K. (Eds), 1996, "Climate Change 1995", Cambridge University Press, Cambridge.

Njau E.C., Int. J. Renewable Energy, 1999, 18, 157.

Njau E.C., Int. J. Renewable Energy, 1996, 7,339.

Njau E.C., J. Climatol., 2006 (In the Press).

Wanner H., La Recherche, 321 (1999) 72.

Njau E.C., Nuovo Cimento C,.29 (2006) 253.

Figure Captions:

FIG. 1: Graphical representation of solar activity form 1700 to 2000 in terms of : (a) Annual number of sunspots (see solid lines), and (b) Relative amplitude of the solid-line variations in (a) as reported in Reg. [1]. On the basis of the curve-fitting methods given Ref. [2], we have fitted a dashed curve along the peaks of the solid-line variations in (a) since 1900.

FIG 2: Time series of he summer monsoon (June-September) rainfall over India (excluding hilly regions) form 1881 to 1980 9see darkened vertical bars) as reported in Ref. [4]. On the basis of the curve-fitting methods given in Ref. [2], we have used dashed lines to sketch out the envelopes of the solid-line variations.

FIG 3: Variations in annual rainfall over Madras, India from 1813 to 1955 (see solid lines) as reported in Ref. [5]. On the basis of the curve-fitting methods given in Ref. [2], we have used dashed lines to sketch out the envelopes of the solid line variations.

FIG 4: Time series of monthly-mean global temperature anomalies (in °C) between May 1963 and April 1988 for the troposphere between the surface and an altitude of about 11 m whose atmospheric pressure in 225 mb (see thin solid lines) as reported in Ref. [4]. The anomalies are taken with respect to the 1963 – 1973 mean conditions. The smooth thick-line curves show the 15-month Gaussian – type filtered values. We have used dashed lines to sketch out the NM and SM variation modes of the thin solid-line variations at periods greater than 9 years on the basis of the curve-fitting methods given in Ref. [2]. Note that meanings of NM and SM are given in the text.

FIG 5: Annual variations of the Troup Southern Oscillation Index (SOI) from 1876 to 1990 (solid lines) as reported in Ref. [13]. The curves about which the SOI variations oscillate have been drawn using heavy dots. Discontinuous lines have been used t sketch out the SM mode (at periods greater than 40 years) of the SOI variations using the curve-fitting methods in Ref. [2].

FIG. 6: Seasonal values of the Troup Southern Oscillation Index (SOl), March –May 1876 through March -May 1995 (solid lines) as reported in Ref. [14]. Discontinuous lines ha\'e been used to sketch out the NM modes of the Sol \"ariations by means of the curve-fitting methods in ,Ref. [2]. Each in\"erted alTOW points at the timing at which an NM mode stops and gives way to the next NM mode.

FIG.7: Same as Fig. 1 but with part (b) displaying relative variation of the frequency of the II-year sunspot cycle" Adapted from Ref. [1].

FIG. 8: A plot of the North Atlantic Oscillation Index (NAOI) from 1864 to 1996 (solid lines) as reported in Ref. [18]. Heavy dotted lines have been used to sketch out the NM and SM patterns whose periods are greater than 24 years by means of

the cuf\'e-fitting methods given in Ref. [2]. Also discontinuous lines have been used to sketch out the NM patterns whose periods are less than 24 years. Each in\"erted arrow shows the timing at which an N~1 or SM (sketched using dotted lines) stops to give way to the next NM or SM"

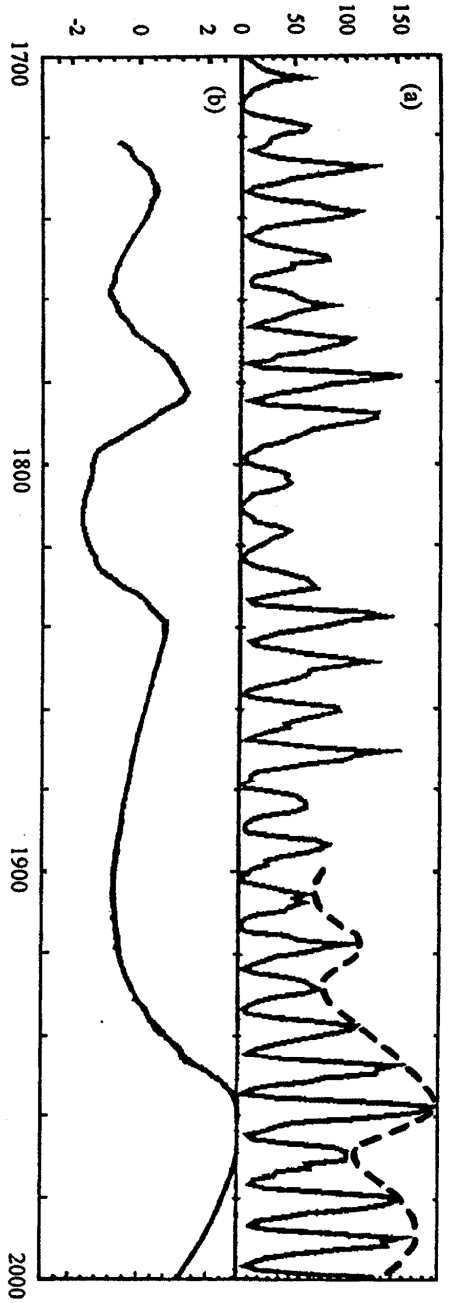

FIG. 1

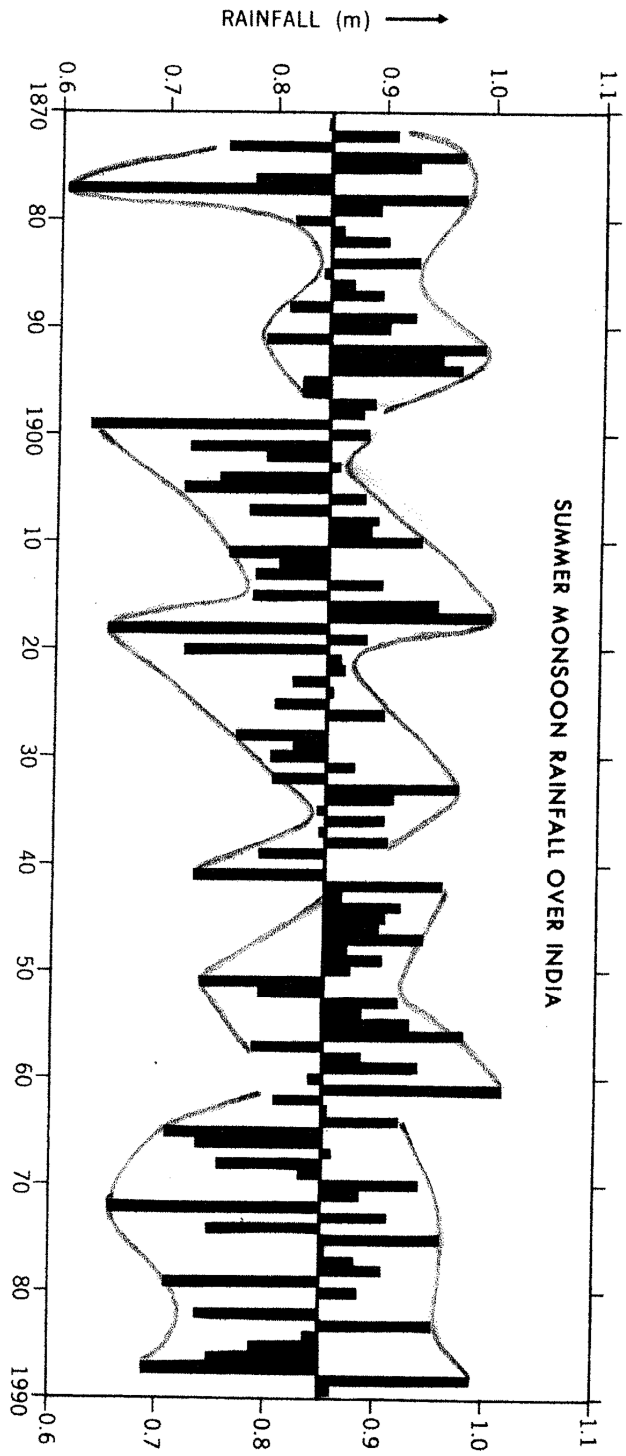
RAINFALL (m)
0.6
0.7
0.8
0.9
1.0
1.1
1870
80
90
1900
10
20
30
40
50
60
70
80
1990
SUMMER MONSOON RAINFALL OVER INDIA

FIG. 2

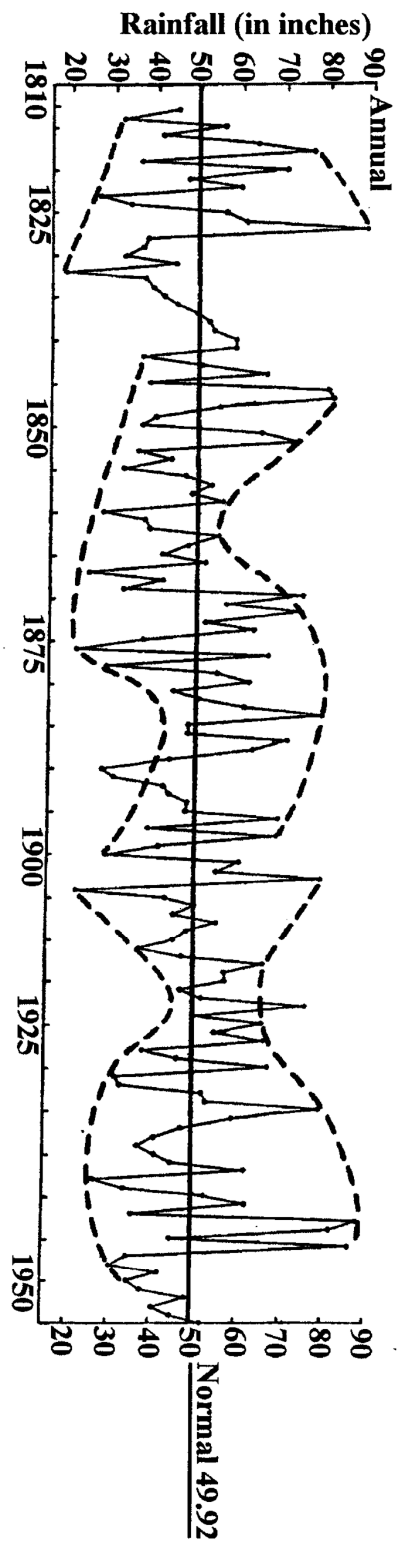
Rainfall (in inches)
Annual
Normal 49.92
1810
1825
1850
1875
1900
1925
1950
20
30
40
50
60
70
80
90

FIG. 3

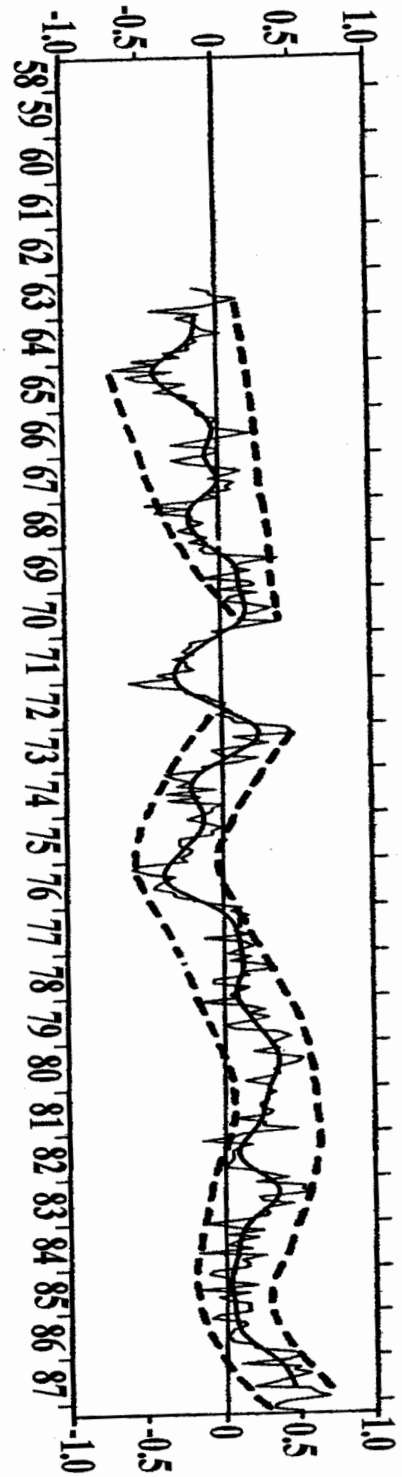
1.0
0.5
0
-0.5
-1.0
58 59 60 61 62 63 64 65 66 67 68 69 70 71 72 73 74 75 76 77 78 79 80 81 82 83 84 85 86 87
1.0
0.5
0
-0.5
-1.0

FIG. 4

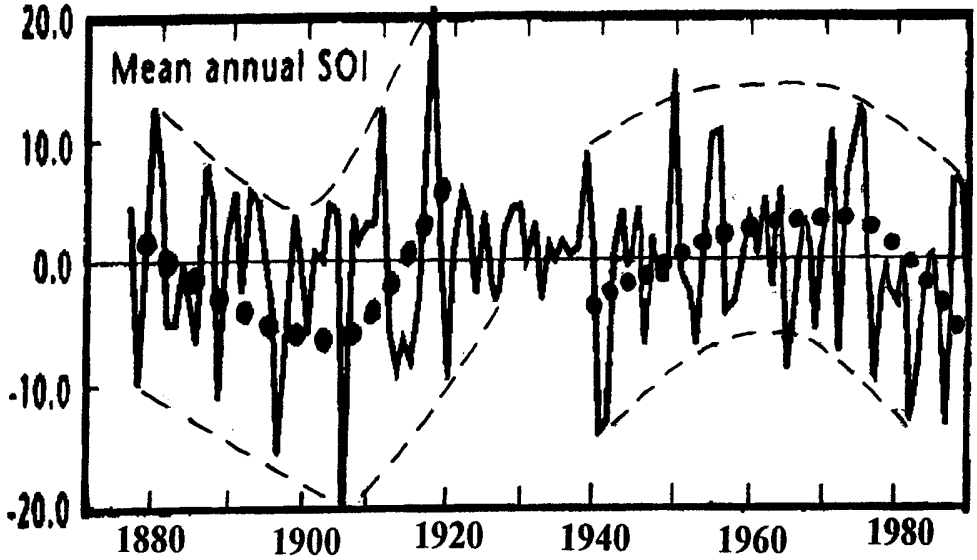
Mean annual SOI
20.0
10.0
0.0
-10.0
-20.0
1880
1900
1920
1940
1960
1980
YEAR

FIG. 5

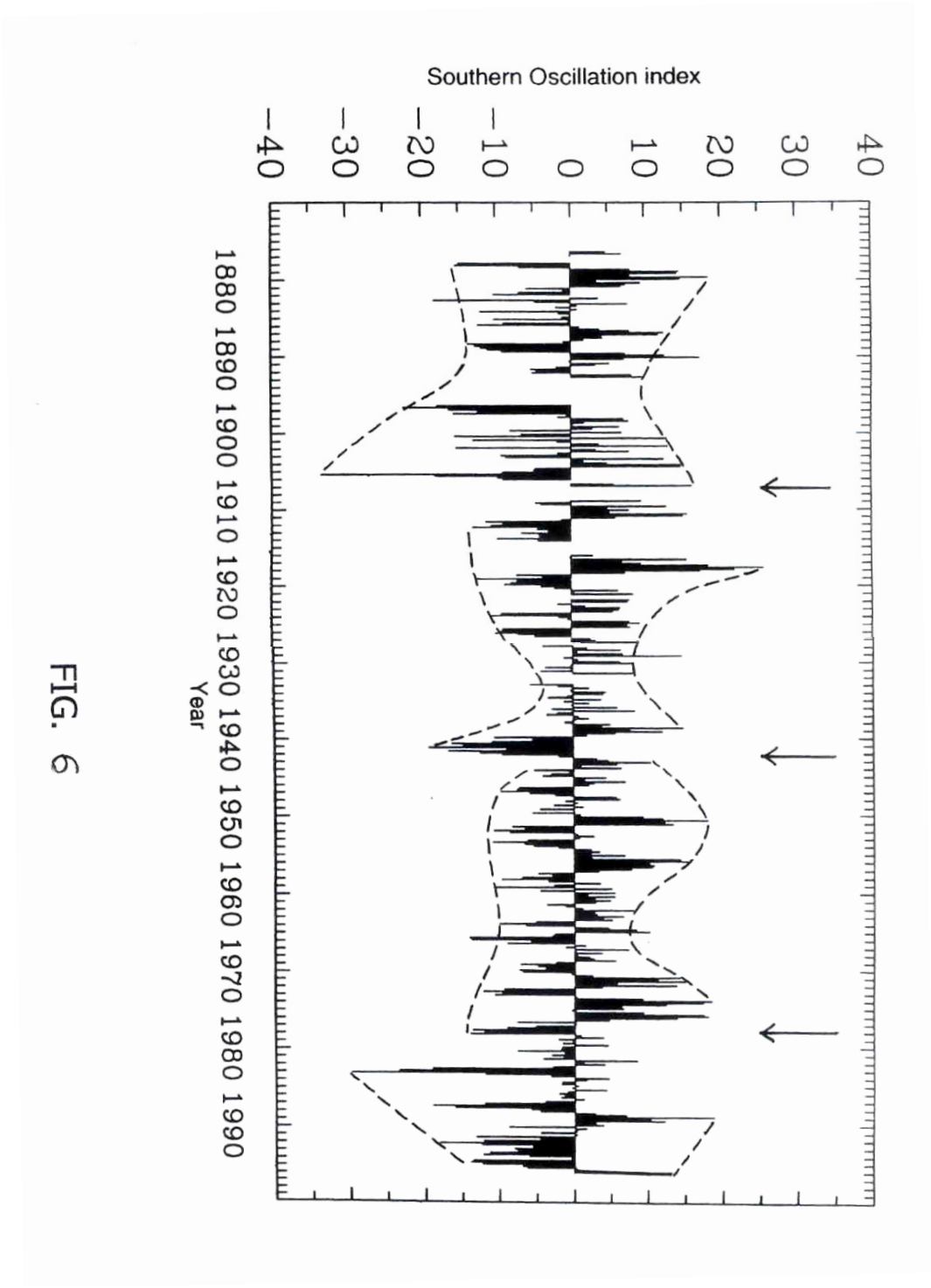
Southern Oscillation index
40
30
20
10
0
−10
−20
−30
−40
1880 1890 1900 1910 1920 1930 1940 1950 1960 1970 1980 1990
Year

FIG. 6

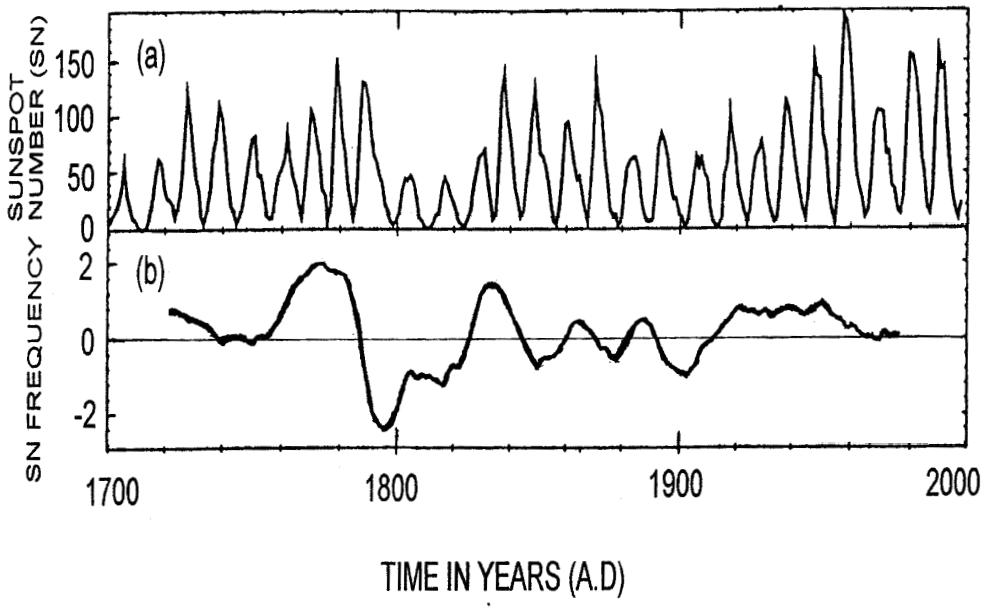
SUNSPOT
SN FREQUENCY NUMBER (SN)
(a)
150
100
50
0
(b)
2
0
-2
1700
1800
1900
2000
TIME IN YEARS (A.D)

FIG. 7

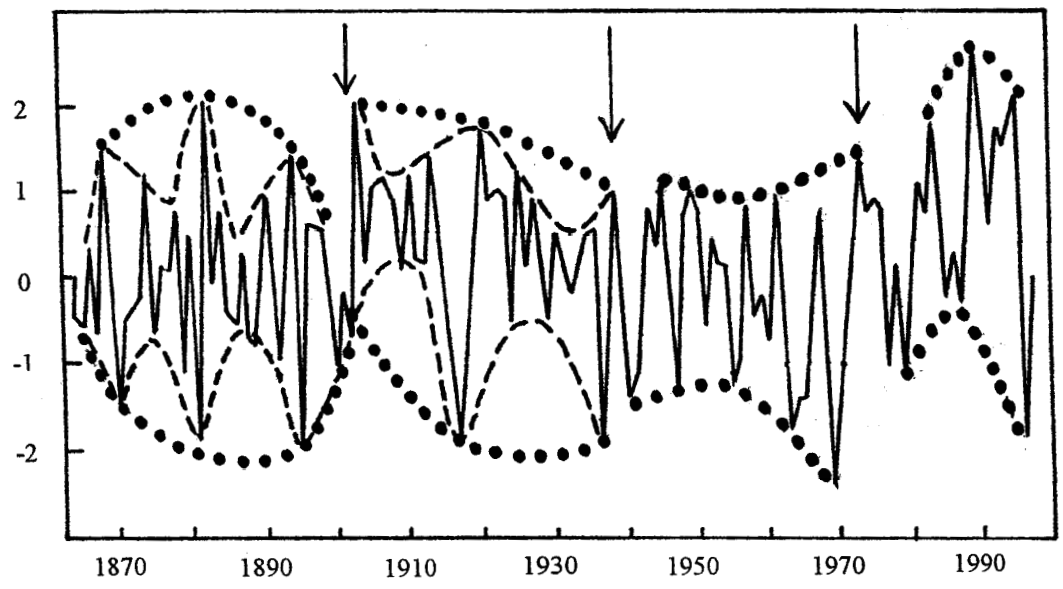
2
1
0
-1
-2
1870
1890
1910
1930
1950
1970
1990

FIG. 8